Statistical Inference of Equivalent Initial Flaw Size Distribution for Fatigue analysis of an Anisotropic Material

Mengke Zhuang,[1, a)] Llewellyn Morse,[2, b)] Zahra Sharif Khodaei,[1, c)] and M.H. Aliabadi[1, d)]

[1)] *Department of Aeronautics, Imperial College London, South Kensington Campus, City and Guilds Building, Exhibition Road, SW7 2AZ, London, UK.*

[2)] *Department of Architecture, University of Ferrara, Via Quartier 8, 44121 Ferrara, Italy*

[a)] *Corresponding author: m.zhuang17@imperial.ac.uk*
[b)] *Electronic mail: mrslwl@unife.it*
[c)] *Electronic mail: z.sharif-khodaei@imperial.ac.uk*
[d)] *Electronic mail: m.h.aliabadi@imperial.ac.uk*

Abstract. A novel methodology for the fatigue life uncertainty quantification of anisotropic structures is presented in this work. The concept of the Equivalent Initial Flaw Size Distribution (EIFSD) is employed to overcome the difficulties in small cracks detection and fatigue prediction. This EIFSD concept is combined with the Dual Boundary Element Method (DBEM) to provide an efficient methodology for modelling the fatigue crack growth. Bayesian inference is used to infer the EIFSD based on inspection data from the routine maintenance of the structure, simulated with the DBEM. A large amount of DBEM simulations were required for the Bayesian inference. Therefore, surrogate models are used as part of the inference to further improve computational efficiency. A numerical example featuring an anisotropic plate is investigated for demonstrating the proposed methodology. When considering a low level of uncertainty in the crack propagation parameters, an error of 0.12% was found between the estimated fatigue life obtained using the proposed method compared to actual fatigue life, and only 0.35% error when considering high level of uncertainty. The application of the estimated fatigue life can be used to determine an appropriate inspection interval for aircraft maintenance.

INTRODUCTION

The use of anisotropic materials in the aviation industry has increased significantly over the last decade due to the advantages they provide in terms of weight and strength. Therefore, being able to perform structural integrity assessments of anisotropic components and estimate their fatigue life is a fundamental requirement for structural integrity management. Ideally, when estimating fatigue life, the growth of an initial crack to some final permissible size could be modelled using a short crack growth model. However, due to the small size of the initial flaw, it is challenging to measure accurately and its growth behaviour is difficult to model due to the heavy influence of the material's micro-structure [1]. These difficulties are especially prominent in anisotropic materials. However, this often results in conservative estimates of fatigue life [2], and over-designed structures that lose the lightweight advantages provided by anisotropic materials. The concept of the Equivalent Initial Flaw Size Distribution (EIFSD) is an efficient fatigue life estimation method that circumvents the above difficulties. EIFSD is not an actual physical quantity, but can be considered as a model parameter used in long crack growth models, such as Paris' law. After the EIFSD has been inferred, it can be used to provide accurate fatigue life estimates for a structure, and can be applied to other structures with the same loading conditions. Fatigue life estimated by EIFSD can be used to avoid over-engineering of components and preserve the weight saving advantages offered by anisotropic materials.

Previous research on the inference of EIFS includes: Bayesian inference was used with Finite Element Method to estimate EIFS by Salemiet [3]. Sankararaman et al. [4] inferred EIFS using Bayesian updating for a cylindrical structure under the presence of various geometric, load, and material uncertainties. Lee et al. [5] conducted several experimental studies considering different probability distributions in the sources of uncertainties. Li et al. [6] inferred EIFS for an anisotropic structure using the modified Kitagawa-Takahashi diagram method. Compare to traditional isotropic materials, anisotropic materials have significantly more uncertainty related to the modelling of fatigue and crack propagation. These uncertainties likely arise due to the manufacturing process and due to the increased complexity associated with modelling crack propagation in anisotropic materials compared to isotropic materials. As a result, determining the EIFSD for anisotropic materials can be challenging.

It can be difficult to collect real inspection data, and it is inefficient to perform experiments on the same structure under several uncertainties. Therefore, in this work, DBEM is used to model the fatigue problem of materials and simulate this inspection data. DBEM is commonly used in modelling crack propagation problems and it only needs to model the external boundary of a structure [7], thereby improving computational efficiency. By combining DBEM and EIFSD methods, EIFSD can be inferred with a smaller quantity of inspection data. Prior work on the combined EIFSD and DBEM approach has been used in a multi-site damage problem [8] and an assembled plate bending problem [9].

In summary, the aim of this work is to extend the previous work for inferring the EIFSD of an anisotropic structure under uncertainties in the geometrical and crack growth parameters. The method presented in this paper is based on previously published work by the same author [10]. Larger coefficient of variance in the uncertainties are included in the example. This is to further verify the proposed method. The methodology of the EIFSD and DBEM will be introduced first, followed by a numerical example with multiple sources of uncertainty.

METHODOLOGY

The Equivalent Initial Flaw Size Approach

EIFS is an 'imaginary' quantity that can be thought of as a parameter in a long crack growth model. EIFS can be defined mathematically by:

$$N = \int_{IFS}^{a_c} \frac{1}{g_s(a)} da = \int_{EIFS}^{a_c} \frac{1}{g_l(a)} da \tag{1}$$

where IFS is the actual initial flaw size and a_c is some critical crack size. $g_s(a)$ is a short crack growth model which can accurately both the long and short crack growth. The EIFS can be found by growing the crack backwards from a_c to its initial state using a long crack growth model $g_l(a)$. A graphical demonstration of the concept of EIFS can be seen in Fig.1. The area under the two curves is the same and represents the number of cycles N required to grow the crack from IFS to a_c using $g_s(a)$ is the same as the number of load cycles required to grow from $EIFS$ to a_c using $g_l(a)$.

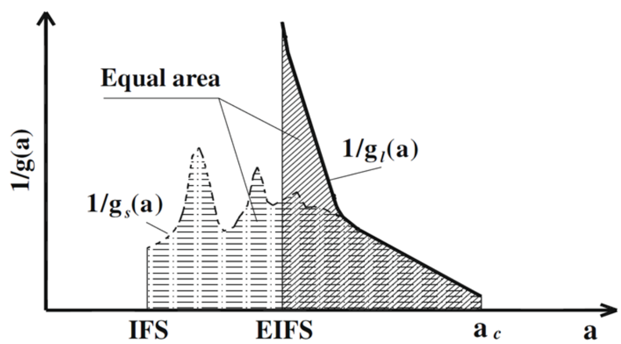

FIGURE 1. Concept of the EIFS and the equivalence between the EIFS and IFS [4].

The DBEM for Anisotropic Materials

In order to simulate the fatigue crack propagation of the structure and estimate the fatigue life, it is necessary to establish a numerical model of the structure. The Dual Boundary Element Method (DBEM) as an alternative version of Boundary Element Method (BEM) which developed specially for modelling the crack were used in this work. In the DBEM, the boundaries S are discretised into N_e elements, and n_e represents the enumeration of each element. The displacement integral equation in a discretised form can be written as:

$$\frac{1}{2} u_i(z') + \sum_{n_e=1}^{N_e} \int_{S_{ne}} T_{ij}(z',z)\, u_j(z) dS = \sum_{n_e=1}^{N_e} \int_{S_{ne}} U_{ij}(z',z)\, t_j(z) dS \tag{2}$$

and the traction integral equation as:

$$\frac{1}{2}t_j\left(z'\right)+\mathrm{n_i}\left(z'\right)\sum_{n_e=1}^{N_e}\int_{S_{n_e}}S_{kij}\left(z',z\right)u_k(z)dS=\mathrm{n_i}\left(z'\right)\sum_{n_e=1}^{N_e}\int_{S_{n_e}}^{\infty}D_{kij}\left(z',z\right)t_k(z)dS \tag{3}$$

where u_i is the displacement at the boundaries and t_j represents the traction at the boundaries. z' and z are the field point and source point. T_{ij}, U_{ij}, S_{kij} and D_{kij} are the fundamental solutions. Details of these fundamental solutions can be found in [7].

One of the reasons that the DBEM is used for modelling crack propagation is that it does not require the re-meshing of the model and the crack propagation path can be calculated automatically. The maximum circumferential stress criterion was used to determine the crack propagation direction [10] and the direction is corrected iteratively by the correction procedure proposed by Lucht [11]. The J-integral method is employed to determine the crack tip stress intensity factors.

Crack Growth Model

The long crack growth model used in this work is the Paris Law. The mathematical formulation of the Paris Law can be written as [12]:

$$N=\int_{a_0}^{a}\frac{1}{da/dN}da \tag{4}$$

where N is the number of load cycles required to grow the crack from a starting length a_0 to some final crack length a, and da/dN is the crack growth rate defined by:

$$\frac{da}{dN}=C(\Delta K_{eff})^m \tag{5}$$

where C and m are the Paris Law constants and exponential that vary depending on the material, ΔK_{eff} is the effective stress intensity factor difference at the minimum and maximum stress level $\Delta K_{eff}=K_{eff}^{max}-K_{eff}^{min}$. Walker's equation defines the relationship between the Paris Law constant C and the stress ratio $R=\sigma_{max}/\sigma_{min}$ as:

$$C=\frac{C_0}{(1-R)^{m(1-\gamma)}} \tag{6}$$

where γ is Walker's equation coefficient and C_0 is the constant evaluated when the stress ratio $R=0$.

Bayesian Inference

Inferring the EIFSD relies upon updating the prior distribution using inspection data to obtain a posterior distribution. The inspection data in this work is in the form of the number of cycles require to reach a critical crack length. A crack is assumed to be detected as soon as it reaches the critical length of $a_{det}=20\ mm$, which is the minimum flaw size that can be detected by the Non-Destructive Inspection (NDI). Assuming that the 'true' EIFSD has a Lognormal distribution with mean μ and standard deviation σ, but the value of the μ and σ are unknown. The purpose of the Bayesian updating is to infer the 'true' EIFSD. Trial pairs of mean and standard deviation $(\hat{\mu}_i,\hat{\sigma}_j)$ within a possible range are defined before the Bayesian Updating. The likelihood that the trial pair $(\hat{\mu}_i,\hat{\sigma}_j)$ is the 'true' EIFSD (μ,σ) given the k^{th}inspection data N_k^{ins} is:

$$\begin{aligned}L\left(\hat{\mu}_i,\hat{\sigma}_j\mid N_k^{ins},\mathbf{Y}\right)&=f_{N|\hat{\mu}_i,\hat{\sigma}_j,\mathbf{Y}}\left(N_k^{ins}\mid\hat{\mu}_i,\hat{\sigma}_j,\mathbf{Y}\right)\\&=\frac{1}{N_k^{ins}\sqrt{2\pi\beta_{ij}^2}}\exp\left(-\frac{\left[\log\left(N_k^{ins}\right)-\alpha_{ij}\right]^2}{2\beta_{ij}^2}\right)\end{aligned} \tag{7}$$

where α_{ij} and β_{ij} are the location and shape parameters of the lognormal distribution $f_{N|\hat{\mu}_i,\hat{\sigma}_j,\mathbf{Y}}$. The values of these two parameters are estimated by propagating the crack with a trial distribution $(\hat{\mu}_i,\hat{\sigma}_j)$ to the critical crack length using Monte Carlo Simulation (MCS). The vector $\mathbf{Y}$ consist of the uncertainties that can affect the fatigue crack growth.

To obtain an accurate likelihood after l inspection data has been used, the likelihood of the trial pair $(\hat{\mu}_i,\hat{\sigma}_j)$ can be written as:

$$L\left(\hat{\mu}_i,\hat{\sigma}_j \mid \mathbf{N}_{1:l}^{ins},\mathbf{Y}\right)=\prod_{k=1}^{l} L\left(\hat{\mu}_i,\hat{\sigma}_j \mid N_k^{ins},\mathbf{Y}\right) \tag{8}$$

and normalized by:

$$L^{norm}\left(\hat{\mu}_i,\hat{\sigma}_j \mid \mathbf{N}_{1:l}^{ins},\mathbf{Y}\right)=\frac{L\left(\hat{\mu}_i,\hat{\sigma}_j \mid \mathbf{N}_{1:l}^{ins},\mathbf{Y}\right)}{\int\int L\left(\hat{\mu},\hat{\sigma} \mid \mathbf{N}_{1:l}^{ins},\mathbf{Y}\right) d\hat{\mu} d\hat{\sigma}} \tag{9}$$

the likelihood of individual $\hat{\mu}_i$ and $\hat{\sigma}_j$ is the true mean and standard deviation is:

$$\begin{aligned} L\left(\hat{\mu}_i \mid \mathbf{N}_{1:l}^{ins},\mathbf{Y}\right) &= \int L^{norm}\left(\hat{\mu}_i,\hat{\sigma} \mid \mathbf{N}_{1:l}^{ins},\mathbf{Y}\right) f_{\hat{\Sigma}|\mathbf{N}_{1:l-1}^{ins},\mathbf{Y}}\left(\hat{\sigma} \mid \mathbf{N}_{1:l-1}^{ins},\mathbf{Y}\right) d\hat{\sigma} \\ L\left(\hat{\sigma}_j \mid \mathbf{N}_{1:l}^{ins},\mathbf{Y}\right) &= \int L^{norm}\left(\hat{\mu},\hat{\sigma}_j \mid \mathbf{N}_{1:l}^{ins},\mathbf{Y}\right) f_{\hat{\mathrm{M}}|\mathbf{N}_{1:l-1}^{ins},\mathbf{Y}}\left(\hat{\mu} \mid \mathbf{N}_{1:l-1}^{ins},\mathbf{Y}\right) d\hat{\mu} \end{aligned} \tag{10}$$

where $f_{\hat{\mathrm{M}}|\mathbf{N}_{l-1}^{ns},\mathbf{Y}}$ and $f_{\hat{\Sigma}|\mathbf{N}_{l-1}^{ins},\mathbf{Y}}$ represent the prior distributions of the inferred mean $\hat{\mu}$ and standard deviation $\hat{\sigma}$ respectively. Initial guesses of these prior distributions are needed for the first iteration of Bayesian inference. The posterior distributions can be updated from the prior terms iteratively. These posterior distributions are given as:

$$f_{\hat{\mathrm{M}}|\mathbf{N}_{1:l}^{ins},\mathbf{Y}}\left(\hat{\mu}_i \mid \mathbf{N}_{1:l}^{ins},\mathbf{Y}\right)=\frac{L\left(\hat{\mu}_i \mid \mathbf{N}_{1:l}^{ins},\mathbf{Y}\right) f_{\hat{\mathrm{M}}|\mathbf{N}_{1:l-1}^{ins},\mathbf{Y}}\left(\hat{\mu}_i \mid \mathbf{N}_{1:l-1}^{ins},\mathbf{Y}\right)}{\int L\left(\hat{\mu} \mid \mathbf{N}_{1:l}^{ins},\mathbf{Y}\right) f_{\hat{\mathrm{M}}|\mathbf{N}_{1:l-1}^{ins},\mathbf{Y}}\left(\hat{\mu} \mid \mathbf{N}_{1:l-1}^{ins},\mathbf{Y}\right) d\hat{\mu}} \tag{11}$$

$$f_{\hat{\Sigma}|\mathbf{N}_{1:l}^{ins},\mathbf{Y}}\left(\hat{\sigma}_j \mid \mathbf{N}_{1:l}^{ins},\mathbf{Y}\right)=\frac{L\left(\hat{\sigma}_j \mid \mathbf{N}_{1:l}^{ins},\mathbf{Y}\right) f_{\hat{\Sigma}|\mathbf{N}_{1:l-1}^{\mathrm{ins}},\mathbf{Y}}\left(\hat{\sigma}_j \mid \mathbf{N}_{1:l-1}^{\mathrm{ins}},\mathbf{Y}\right)}{\int L\left(\hat{\sigma} \mid \mathbf{N}_{1:l}^{\mathrm{ins}},\mathbf{Y}\right) f_{\hat{\Sigma}|\mathbf{N}_{1:l-1}^{\mathrm{ins}},\mathbf{Y}}\left(\hat{\sigma} \mid \mathbf{N}_{1:l-1}^{\mathrm{ins}},\mathbf{Y}\right) d\hat{\sigma}} \tag{12}$$

where $f_{\hat{\mathrm{M}}|\mathbf{N}_{1:l}^{ns},\mathrm{Y}}$ and $f_{\hat{\Sigma}|\mathbf{N}_{1:l}^{ins},\mathrm{Y}}$ are the posterior distributions. The estimation of mean and standard deviation of EIFSD is obtained by applying:

$$\mu_{BU,1:l}=\mathrm{E}(\hat{\mathrm{M}})=\int \hat{\mu} f_{\hat{\mathrm{M}}|\mathbf{N}_{1:l}^{\mathrm{ins}},\mathbf{Y}}\left(\hat{\mu} \mid \mathbf{N}_{1:l}^{\mathrm{ins}},\mathbf{Y}\right) d\hat{\mu} \tag{13}$$

$$\sigma_{BU,1:l}=\mathrm{E}(\hat{\Sigma})=\int \hat{\sigma} f_{\hat{\Sigma}|\mathbf{N}_{1:l}^{\mathrm{ins}},\mathbf{Y}}\left(\hat{\sigma} \mid \mathbf{N}_{1:l}^{\mathrm{ins}},\mathbf{Y}\right) d\hat{\sigma} \tag{14}$$

It is expected that the estimated $\mu_{BU,1:l}$ and $\sigma_{BU,1:l}$ will approach the 'true' values of μ and σ when more inspection data is used.

NUMERICAL EXAMPLE

A numerical example featuring an anisotropic plate with a centred hole and a crack was investigated to demonstrate the proposed method for the inference of EIFSD. The geometry is shown in Fig. 2. Uniform stresses were applied on the top and bottom boundaries. Assuming that the principal axis of anisotropy is oriented at an angle $alpha$ to the horizontal. A fictional material property that is a function of the ratio between Young's modulus $\psi = E_1/E_2$ was used. Poisson's ratio $\nu_{12} = 0.29$, shear modulus $G_{12} = 789\ MPa$, material constant $\gamma = 0.68$ [9]. Young's modulus is represented by $E_1 = G_{12}(\psi + 2\nu_{12} + 1)$ [13]. The location of the starting crack size a_0 is shown in region B and it is assumed to be initialised along the E_1 direction. The 'true' EIFSD is assumed to have a lognormal distribution of $\theta_{act} \sim lnN(6.0, 0.6)\ mm$.

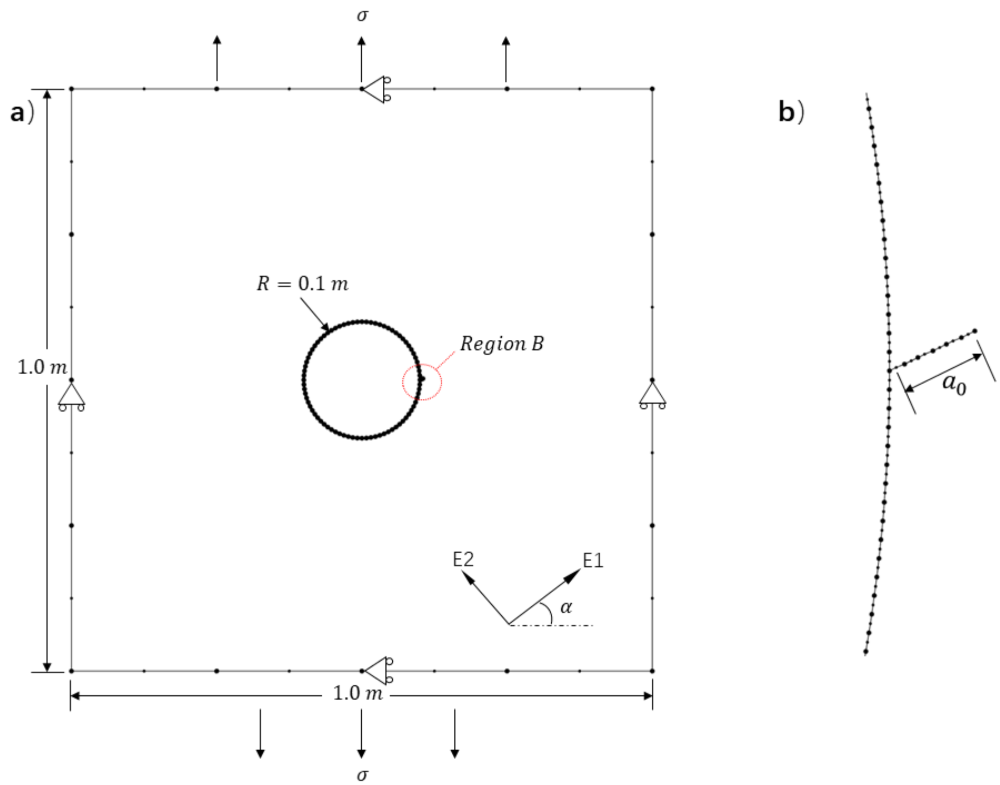

FIGURE 2. Sub-figure (a): The boundary element mesh of the structure and the boundary conditions. Sub-figure (b): The zoom-in demonstration of the starting crack.

The structure consists of an outer boundary, an inside circular boundary, and the crack. Each edge of the outer boundary is meshed by four elements each, and the inner boundary is composed of 160 elements. Fig.2 shows the mesh for the starting crack. The starting crack a_0 of length 3 mm mm is composed of three elements for each crack surface. When modelling the growth of the crack, one element is added during each crack increment to each crack surface at the crack tip.

In this work, the inspection data is numerically created using the DBEM. The parameters that affect the crack growth are the Young's modulus ratio ψ, the orientation of the axis of anisotropy α, Paris law constantsC_0 and m, maximum loading stress σ_{max} and stress ratio $R = \sigma_{min}/\sigma_{max}$. These parameters are assumed to have lognormal distributions. To determine the robustness of the proposed method, two uncertainty levels for each crack growth parameter are investigated: low and high. The distribution and coefficient of variation (COV) assigned to each crack growth parameter are listed in the Tab. I. For each inspection simulation, the 'true' EIFSD is randomly sampled to generate a starting crack size, while the value of each crack propagation parameters are randomly selected from their distributions. For each inspection, the number of cycles required to grow a starting crack size to a_{det} was recorded.

TABLE I. Uncertainties in the parameter presented in the fatigue crack growth.

Variable	Description	Distribution	Mean	CoV Low	CoV High
C_0	Paris law Constant	Lognormal	$1.027 \times 10^{-9} \frac{m/cycle}{(MPa\sqrt{m})^m}$	0.02	0.05
m	Paris law exponent	Lognormal	2.389	0.01	0.02
σ_{max}	Maximum applied stress	Lognormal	25 MPa	0.02	0.05
R	Stress ratio	Lognormal	0.3	0.02	0.05
ψ	Ratio of Young's modulus	Lognormal	0.15	0.02	0.05
α	Anisotropic principal axis orientation	Lognormal	25^o	0.02	0.05

TABLE II. The statistical error in stress intensity factors and fatigue life between the actual DBEM and the surrogate model.

Model	RRSE(%)	MAPE(%)	MAE	RMSE	R^2 (%)
K_{eff}	4.59	0.35	0.058 $MPa\sqrt{m}$	0.089 $MPa\sqrt{m}$	99.7
N	6.33	2.74	494 $cycles$	599 $cycles$	99.6

Surrogate model

As described in the previous section, 60×60 trial pairs of mean and standard deviation were assumed and applied in Monte Carlo Simulation for the estimation of the distribution $f_{N|\hat{\mu}_i,\hat{\sigma}_j,\mathbf{Y}}$ in Eq.7. Overall 1×10^6 samples were used for each trial pair to estimate this distribution with high accuracy. The computational cost is expensive when simulating the structure using the DBEM for large amount of samples. Instead, a stochastic Kriging model was used to replace the DBEM in MCS. The output from the model is the effective SIF K_{eff}, once the effective SIF is determined, the number of cycles for crack growth can be obtained by using the Paris Law in Eq.5. When training a stochastic Kriging model, the values of material property ψ, crack propagation length a_0, a were provided as inputs, such that:

$$K_{eff} = f^{kriging}(\psi, \alpha, a_0, a) \tag{15}$$

where $f^{kriging}$ is the surrogate model (stochastic Kriging model) that estimates the crack tip effective SIF when growing the crack from the starting length a_0 to a final length a. Once the surrogate model for the K_{eff} is obtained, the Paris Law can be applied to create the surrogate model for the fatigue cycles N to grow the crack from a_0 to a.

Overall 342 points were used to train the surrogate model and 6.7 hrs were required for the training. An accuracy test was conducted to determine the error between the DBEM and the obtained surrogate models. Overall 2700 testing points of K_{eff} and N were generated directly from the DBEM and the values were compared to that given by the surrogate model. A graphical presentation of the entire stochastic model is difficult to show since the model has four inputs and an output. Therefore, only a 3-D example of the model when $\psi = 0.18$ and $\alpha = 24°$ for K_{eff} and N is given in Fig.3, the corresponding testing points are shown in black dots. The statistical errors between the stochastic models and the testing points were evaluated and shown in Tab.II. The errors between the surrogate model and the results from the DBEM have very low values.

To determine the efficiency of the surrogate model, a study was carried out. It was found that the average CPU time required to estimate one value of K_{eff} was 3.73 s for the DBEM, while it was 0.0156 s for the surrogate model, a decrease by a factor of around 239.

Bayesian Inference of EIFS

The proposed inference methodology described earlier is applied here to the geometry shown in Fig.2. To demonstrate the robustness of the proposed method, two sources of the uncertainties were considered:

1. **The quality of the prior distribution:** An initial guess of the prior distribution should be given to start the Bayesian Updating as shown in Eq.12 and 11. This prior distribution is normally chosen according to previous experience and engineering judgment. Two quality levels of the prior distributions were tested to show the robustness of the inference methodology. The quality levels are referred to here as 'good' and 'poor' prior distributions. The quality of a prior distribution is defined by its 'closeness' to the 'true' EIFSD. The 'good' prior distribution is $(5mm, 0.5mm)$, while 'poor' prior distribution is $(0.5mm, 1.5mm)$.

2. **The uncertainty level of the crack growth parameters:** Two levels of uncertainties, 'low' and 'high', are given in Tab. I in terms of the coefficient of variation (COV);

The convergence of the mean and standard deviation is shown in Fig. 4 and 5 under low and high levels of uncertainty, respectively. Fig. 4 shows, for the 'low' uncertainty case, that after using the data from 123 inspections, the value of the mean achieves convergence at 5.97 mm. The data from around 77 inspections are required to bring the mean close to the 'true' mean (6 ± 0.1 mm). The difference between the inferred mean and the 'true' mean is 0.56%. The value of standard deviation achieves convergence at around 265 inspections. The value of the inferred standard deviation is

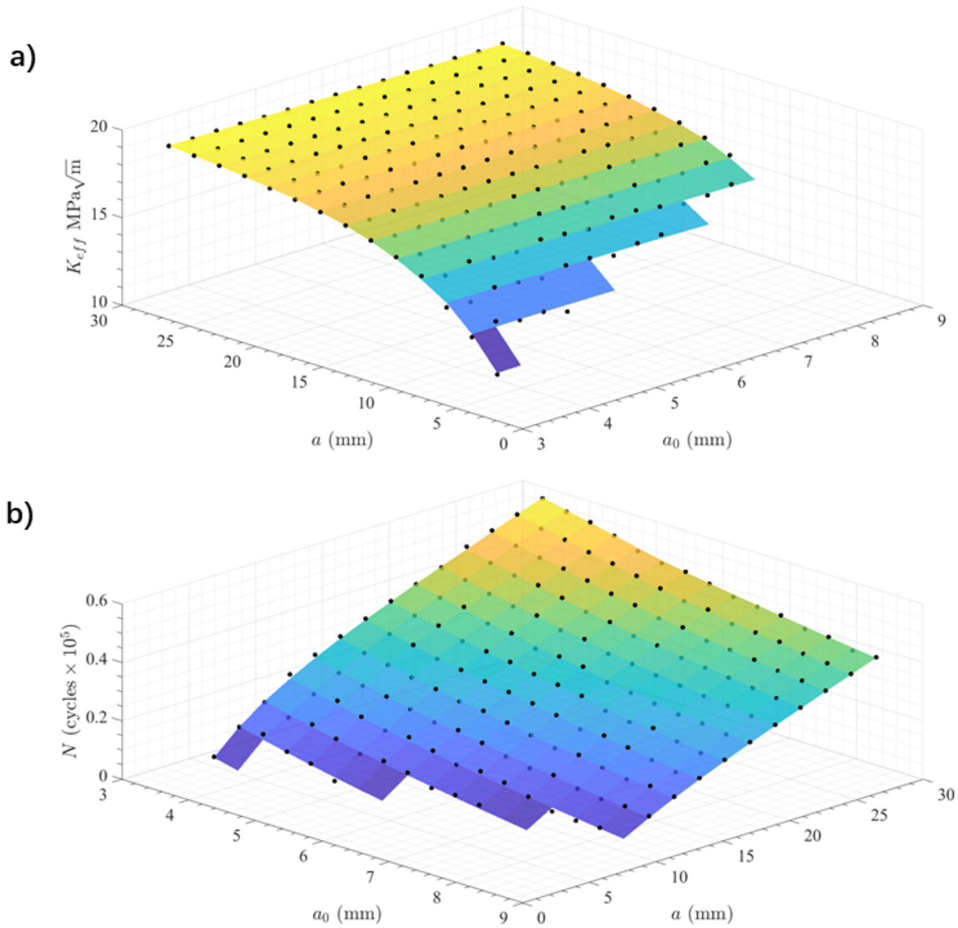

FIGURE 3. Surface plot showing the results of stochastic Kriging model evaluation comparing to the test dataset when $\psi = 0.18$ and $\alpha = 24°$. Sub-figure (a) surrogate model for K_{eff} and sub-figure (b) surrogate model for N.

0.619 *mm* with an error of 3.11%. The quality of the prior estimation has very little impact on the inferred value, a noticeable impact can only be observed when a limited amount of inspections are available (less than 80 inspections).

The convergence for in the 'high' uncertainty case is shown in Fig. 5 and similar convergence pattern can be observed. The mean converged at about 183 inspections of the data was used with an error of ± 0.1 *mm* to the 'true' mean (6 *mm*). The values of the mean after 700 inspections achieve the same value as in the 'low' uncertainty case. The standard deviation achieves an error of 4.83% (0.629 *mm*) after 790 inspection data were used. The initial guess quality has a small effect on the convergence of the mean. However, the convergence behaviour for the standard deviation is greatly affected when the data from a low number of inspections is used (under 170 inspections), but is less affected when more inspection data is available. It is within expectations that for higher uncertainty level, more inspection data is needed to achieve convergence.

Application of the inferred EIFSD

Aircraft components should be routinely inspected to avoid failure of the structure. The inspection interval of a component is usually determined according to its fatigue life, which can be determined by propagating the crack from the inferred EIFSD to a critical size $a_{critical}$. This demonstrates how employing EIFSD inference could be advantageous for maintenance.

A showcase of how the EIFSD can be applied tp determine fatigue life is demonstrated using the same example from Fig.2 and the same uncertainties in the fatigue crack growth parameter. Since the same example is used, the

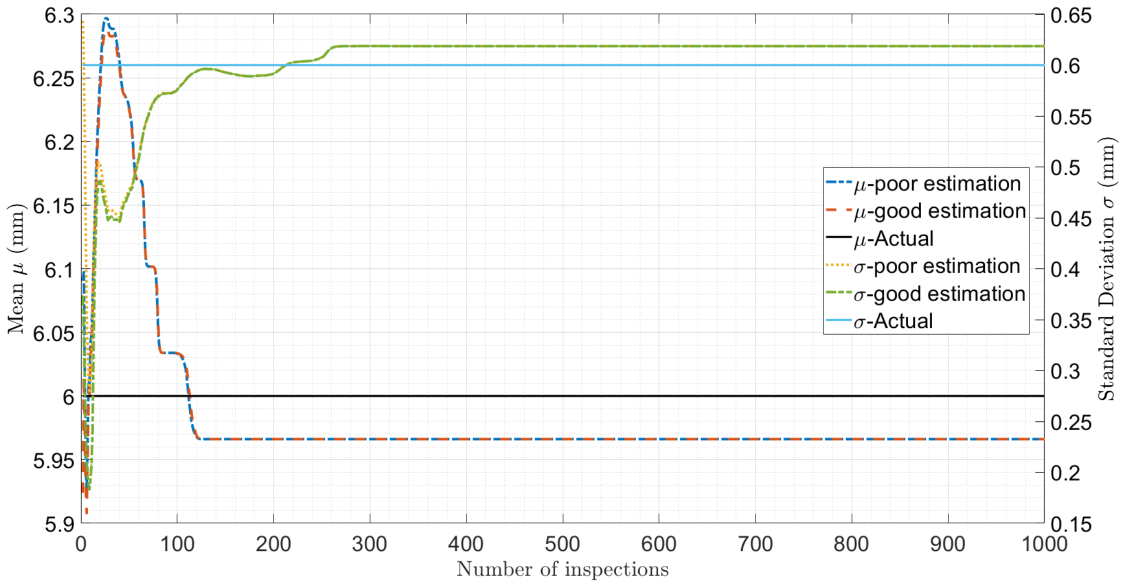

FIGURE 4. Convergence behaviour for the 'low' level of uncertainty.

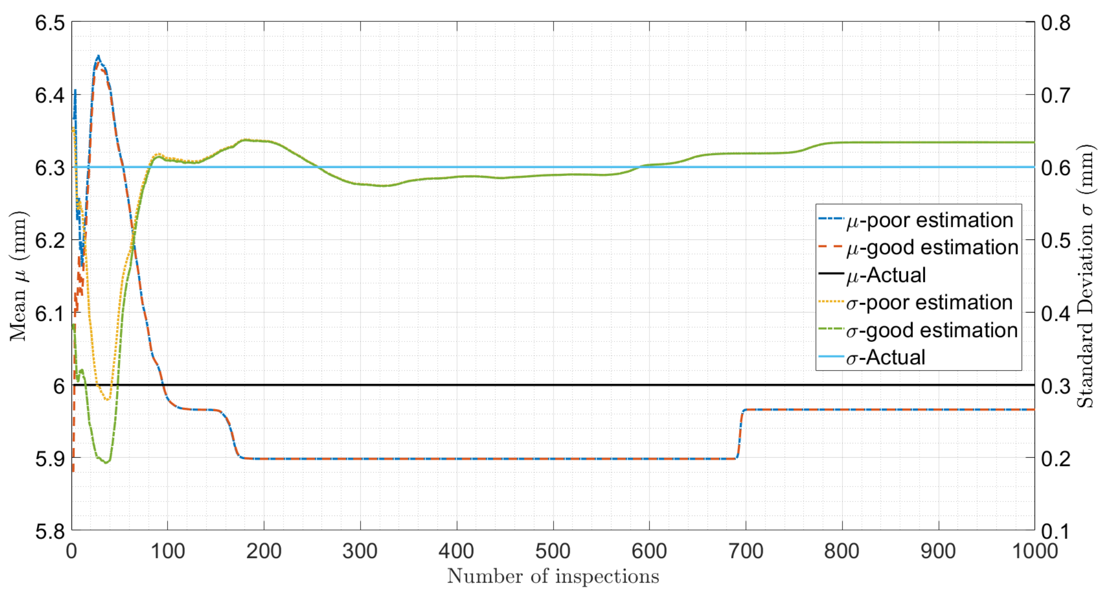

FIGURE 5. Convergence behaviour for the 'high' level of uncertainty.

inferred EIFSD from Bayesian updating in the last section can be applied for estimating the fatigue life via Monte Carlo Simulations (MCS). The critical crack size is assumed to be $a_{critical} = 35\ mm$ as an example and the number of cycles required to grow the crack from its EIFSD to $a_{critical}$ is recorded. Overall 1×10^6 samples were used in MCS. The initial crack size, uncertainties in the geometry and the parameters that are affecting the crack growth are randomly sampled for each simulation. The values of the location and shape parameter α and β can be found by fitting the results obtained from the MCS to a lognormal distribution.

The obtained results from the Bayesian updating under 'high' and 'low' levels of uncertainty were used for MCS. The criterion used to determine the inspection interval largely depends upon engineering judgment. The hypothesis

TABLE III. The results of the distribution of the fatigue life in the form of $lnN(\alpha,\beta)$ obtained using the Monte Carlo simulation. Assuming that the structure need to ensure that the failure chance of less than 2%.

	Lognormal		
EIFSD (mm)	α	β	N_{ins} ($\times 10^4 cycles$) required for $P_{failure} \leq 2\%$
$\theta_{low} \sim lnN(5.9661, 0.6186)$	11.211	0.0751	6.339
$\theta_{high} \sim lnN(5.9661, 0.6289)$	11.215	0.1868	5.059
$\theta_{act\_low} \sim lnN(6.0, 0.6)$	11.209	0.0737	6.346
$\theta_{act\_high} \sim lnN(6.0, 0.6)$	11.213	0.1853	5.077

used in this work is that the component should be inspected at N_{ins} so that the structural failure chance is less than 2%. As such, the obtained fatigue lifetime can be used to estimate N_{ins}. The fatigue life distributions and the corresponding N_{ins} are given in Tab.III.

It can be seen from Tab.III, that a reduced inspection interval is needed when there exists a higher level of uncertainty in the crack propagation. This means that inspections should be conducted more frequently and the overall cost of inspection will increase. Furthermore, it can be seen that the number of cycles for failure are very similar (0.12% difference at low uncertainty and 0.35% at high uncertainty) between the case where the actual EIFSD was used versus the case where inferred EIFSD was used. This demonstrates that the proposed EIFS inference methodology is capable of accurately estimating the true EIFS and that it can be used to accurately determine inspection intervals.

CONCLUSION

A novel methodology for the fatigue life uncertainty quantification of anisotropic structures was presented in this work. This methodology employed the concept of the Equivalent Initial Flaw Size Distribution (EIFSD), the Dual Boundary Element Method (DBEM), and surrogate modelling, to overcome the challenges associated with modelling the growth of small cracks and to provide an efficient methodology for fatigue crack growth modelling. Statistical inference, in the form of Bayesian inference, was used to infer the EIFSD using simulated aircraft inspection data. To demonstrate the proposed novel methodology, a numerical example featuring an anisotropic square plate with a crack was investigated. To test the robustness of the proposed method, two levels of uncertainty were considered. Convergence results show that the EIFSD was accurately inferred within 5% error for both levels of uncertainty. The quality of the estimated prior distribution only has a significant effect when the data from a small number of inspections are available. Once the EIFSD has been inferred, inspection intervals can be accurately determined. This shows one potential application of the inferred EIFSD in the maintenance of aircraft.

REFERENCES

1. A. Navarro and E. R. de los Rios, Philosophical Magazine A **57(1)**, 15–36 (1988).
2. W. S. Johnson, Procedia Engineering **2(1)**, 47–58 (2010).
3. M. Salemi and H. Wang, Journal of Infrastructure Preservation and Resilience **1(1)**, 2 (2020).
4. S. Sankararaman, Y. Ling, and S. Mahadevan, International Journal of Fatigue **32(10)**, 1689–1700 (2010).
5. Y. Lee, J. Park, and D. Lee, Structural Health Monitoring **21**, 1396–1406 (2022).
6. F. Li, Z. Wen, Z. Wu, H. Pei, and Z. Yue, International Journal of Fatigue **160**, 106886 (2022).
7. M. H. Aliabadi, *The Boundary Element Method: Applications in solids and structures*, Vol. 2 (John Wiley and Sons, 2002).
8. L. Morse, Z. S. Khodaei, and M. H. Aliabadi, Journal of Multiscale Modelling **08**, 1740001 (2017).
9. L. Morse, Z. S. Khodaei, and M. H. Aliabadi, Engineering Fracture Mechanics **238**, 107271 (2020).
10. M. Aliabadi and P. Sollero, Composites Science and Technology **58**, 1697–1703 (1998).
11. T. Lucht and M. Aliabadi, International Journal of Fracture **143(2)**, 195–202 (2007).
12. K. Walker and W. Hu, in *Conference: Proceedings of twenty-fourth 2007 ICAF Symposium* (Naples, Italy, 2007).
13. P. Sollero and M. Aliabadi, International Journal of Fracture **64**, 269–284 (1993).
14. S. A. Nor Mohamed, E. S. Zainudin, S. M. Sapuan, M. A. Md. Deros, and A. M. Arifin, BioResources **16(3)**, 4963–4985 (2021).
15. M. Zhuang, L. Morse, Z. Sharif Khodaei, and H. Aliabadi, M, International Journal of Fatigue **158**, 106702 (2022).
16. B. Zheng and M. Dawood, Composite Structures **164**, 158–169 (2017).